FACULTY OF PSYCHOLOGY AND EDUCATIONAL SCIENCES

Analysis of beta bursts induced by deviant tone

Andreas De Bleser
Student number: 01509904

Supervisor: Daniele Marinazzo

A project in partial fulfilment of course ‘Case studies in analysis of experimental data’

Academic year: 2019 – 2020

GHENT UNIVERSITY

The functional role of beta oscillation (13-30Hz) has been studied for a long time. The beta oscillations occur during stable postures and disappear during movement, consequently, It has been proposed that these oscillations indicate a state of status-quo of the sensorimotor system (Engels & Fries, 2010). The beta oscillations are a signature an active process that promotes the existing posture while preventing the neural processing of new movements in the sensorimotor cortex. This functional description of beta oscillations corresponds with the increased beta oscillations found in patients with Parkinson's disease (Holt, et. al., 2019), which is characterized by rigidity and slow movement. However, beta oscillations are not only observed in the sensorimotor cortex, but also the prefrontal cortex (PFC) during executive control of action (Kamarajan et. al., 2004), working memory, and preventing distractions. The basal ganglia also show an increase of beta oscillations as a result of sensory cues (Leventhal et. al., 2012).

Using a delayed match-to-sample task, Lundqvist et. al. (2018) showed that beta oscillations are decreased during the encoding phase, moderated during the delay phase, and strongly increased after the response. It has been suggested that these increased beta oscillation after the response reflect a 'clear-out' of the working memory because the encoded information was no longer needed and new information needs to be stored (Schmidt et. al., 2019). Correspondingly, an increase in beta oscillations after successfully stopping a movement in a stop-signal task has been found in the right frontal areas (Wagner et. al., 2018). It has been proposed that encountering unexpected events could be seen as an alternate form of interrupting working memory because unexpected events induce similar beta oscillations in the right frontal areas to induced activity elicited by successfully stopping a movement. In other words, the ongoing thought, or action plan is unnecessary and therefore removed from the working memory.

In sum, beta oscillations are related to a variety of cognitive functions in different brain regions. In most studies, neural oscillations are analyzed using methods based on the Fourier and Hilbert transform by decomposing the signal into sinusoids. However, brain rhythms are not strictly sinusoidal, nor stationary, and consequently are these conventional methods unable to capture non-sinusoidal oscillatory features and the non-stationarities of low-frequency oscillations. Besides, the conventional analyses are susceptible to spurious phase-amplitude and cross-frequency coupling because it does not account for these non-stationary oscillations (Gerber et. al., 2016; Lazona-Soldevilla et. al., 2016). Instantaneous measures of oscillatory amplitude, phase, and

frequency are widely used to estimate the time-varying properties of the oscillations. However, these instantaneous measures are not directly measured in the raw recording, instead, they are computed based on a transformed version of the data which is filtered to a narrow sinusoidal frequency band (i.e. narrow-band analysis). As such, the following study will investigate the increase of beta oscillations in the frontal brain area after an unexpected auditory tone using cycle-by-cycle measures, a time-domain approach complementary to the conventional frequency-domain methods. This method analyses amplitude, period, and waveform symmetries for each cycle, and these cycle-by-cycle measures are computed directly on points of the time series and do not rely on the transformation of the raw data as is the case in conventional analyses.

Material & Methods

Dataset and software

The auditory brainstorm dataset (Tadel et. al., 2011) contains the data from one participant, which completed two runs. Each runs consists out of 200 regular beeps (440 Hz) and 40 deviant (554.4 Hz) beeps. The participant was instructed to press a button when detecting a deviant beep with the right index finger. The magnetoencephalography (MEG) data was acquired using a CTF 275 system and was collected at 2400 Hz, and was low-pass filtered at 600 Hz. The data consisted of recordings from 340 channels: 274 MEG axial channels, 26 MEG reference channels, 2 EEG electrodes (Cz and Pz), 1 stimulus channels, 1 audio channel, 1 response channel, 1 ECG channel, 2 EOG channels, 12 head tracking channels, and 20 unused channels. Data was analyzed Python (version 3.7.6) using the MNE toolkit (version 0.19), bycycle package (version 0.1.2), and neurodsp (version 2.0).

Cycle-by-cycle burst detection

Preprocessing. Annotated noisy channels were removed from the data, and saccades were removed from the raw data using signal space projection (SSP). Subsequently, the continuous data in which the deviant tone appears is epoched and resampled to 200 Hz. Pre-tone epochs are created using a -500 - 0 ms time window locked to the tone, and after-tone epochs are created using a 0 - 500 ms time window. The frontal sensors are picked for further analysis to save computational memory.

Cycle computation. The cycle-by-cycle analysis is used to quantify time-domain features for each cycle. The first step in a cycle-by-cycle analysis of oscillations is the segmentation of the signal into cycles, as such the putative peak and troughs need to be identified. In order to do is the epoched signal is first passed through a low-pass filter of 40 Hz to remove slow transient high-frequency activity. Subsequently, the data is filtered in the band of interest (13-30 Hz, the beta band). Next, the time points of the rise and decay zero-cross are identified and the midpoints of the rise and decay flanks are computed (Fig. 1). These extrema and flank midpoints can be used to estimate a phase time series.

The second step consists of computing cycle features: the amplitude, the period, the rise-decay symmetry, and peak-trough symmetry. First, the amplitude of a cycle is the average voltage between trough and two peaks. Second, the period of a cycle is the time between two peaks. Third, the rise-decay symmetry (rdsym) is the fraction of the period that was composed of the rise time (e.g., rdsym = 0,5 indicates an equal duration of rise and decay). Last, the peak-trough symmetry (ptsym) is the fraction of the period, encompassing the previous trough and current peak, which was composed of the peak (e.g., ptsym = 0,5 indicates an equal duration of peak and through). These features are compared across all cycles in a signal in order to compare oscillation properties.

The final steps determine the oscillatory burst periods. Oscillatory bursts are time periods in which consecutive cycles have similar amplitudes, periods, and rise and decay flanks. After visual inspection, a threshold of 0.4 for amplitude consistency was applied, a threshold of 0.5 for the period consistency, and a threshold of 0.8 for the monotonicity was applied. An additional threshold of 0.2 for the amplitude fraction as such the cycle amplitude must be above the twentieth percentile in order to prevent aperiodic portions of the signal to be considered part of an oscillation (Fig. 2A - E).

Analysis & Results

Comparison frontal sensors pre- and post-cue

The cycle features were computed for each oscillatory beta burst in the signal obtained by the frontal sensors on deviant trials. Differences in amplitude, period, ride-decay symmetry, and peak-trough symmetry were analyzed by a one-way multivariate analysis of variance (MANOVA) with timing as factor (pre cue, post cue). A significant effect of timing on beta amplitude ($F(2,205) = 68.248$, $p < 0.001$) (Fig. 3A) and period

($F(2,205) = 49.153$, $p < 0.001$) (Fig. 3B) was found. The effect of timing on rise-decay symmetry ($F(2,205) = 1.656$, $p = 0.19$) (Fig. 3C) and peak-trough symmetry ($F(2,205) = 0.255$, $p = 0.77$) (Fig. 3D) did not reach significance levels.

Comparison occipital area and frontal area

For beta oscillation in both, occipital, and frontal areas, were the cycle feature computed. In the pre-cue time period there was a significant difference in the amplitude of beta oscillation ($F(2,100) = 4.288$, $p < 0.05$), and period ($F(2,100) = 29.261$, $p < 0.001$) between signals from the frontal and occipital sensors. However no significant differences were found for rise-decay symmetry ($F(2,100) = 1.078$, $p = 0.34$) and peak-trough symmetry ($F(2,100) = 0$, $p = 1.00$). In the post-cue period there was no significant difference between the amplitude of the beta oscillation in the signal of frontal and occipital sensor ($F(1,100) = 0.006$, $p = 0.93$) and peak-trough symmetry ($F(1,100) = 3.14$, $p = 0.079$). Difference in period ($F(1,100) = 15.95$, $p < 0.001$) and rise-decay symmetry did reach significance levels ($F(1,100) = 7.30$, $p < 0.008$) (Fig. 4).

Visual comparison of cycle-by-cycle and dual amplitude method

Oscillatory beta bursts were computed using two different algorithms: the aforementioned cycle-by-cycle algorithm, and the dual amplitude threshold algorithm. The amplitude threshold algorithm imposes a low and high amplitude threshold on the median averaged signal. Visual comparison of the detected burst (Fig. 5) suggests that the cycle-by-cycle algorithm and therefore the chosen thresholds were accurate since all the oscillations detected by the dual-threshold method were detected by the cycle-by-cycle algorithm. However, the cycle-by-cycle algorithm was able to detect more beta oscillations at a various range of amplitudes.

Discussion

In summary, an increase in the amplitude, and a decrease in period of beta oscillations were found after the participant perceived a deviant auditory tone. The effects of an unexpected, deviant tone on frontal beta oscillations are similar to the effects found in Wagner et. al. (2018) and provide further support for the idea that beta oscillations function as a ‘clear out’ of the working memory (Lundqvist et.al., 2016), in the frontal areas of the brain, after encountering unexpected events. In the future source localization could help in the selection of the most informative sensors, as it has been suggested that the right inferior frontal gyrus is a critical area for stopping (Aron

et. al., 2014). The notion that an increase in beta oscillations is situated frontally, is supported by the comparison of oscillations in frontal and occipital sensors. More specifically, before the presentation of an unexpected event, there is significantly less beta oscillation in the frontal than in the occipital areas, however, after the presentation of the deviant tone, beta oscillations in the frontal area increase to similar levels as in the occipital area.

The cycle-by-cycle used in this study seems to be compatible with other methods aiming to quantify time-domain oscillatory features, as suggested by the visual comparison of the cycles detected by the dual-amplitude threshold algorithm and the cycle-by-cycle algorithm. More specifically, results in the dual-amplitude correspond with the cycle-by-cycle algorithm, however, the cycle-by-cycle algorithm seems to perform better since it is more sensitive towards oscillations at a various range of amplitudes. This increased sensitivity, however, comes at the cost of an increased hyperparameter selection which requires experiences with data to acquire sensible results. That said, it should be noted that hyperparameter selection is not a problem uniquely appearing in the cycle-by-cycle algorithm. In summary, the cycle-by-cycle algorithm is preferable over dual amplitude threshold. In addition, the cycle-by-cycle algorithm provides measures of symmetry (e.g., peak-trough symmetry is used as a measurement of sharpness) allowing further specification on how the beta oscillations are related to unexpected events. More specifically, the results of this study suggest that an unexpected event only affects the amplitude, and the period of the beta oscillations in the frontal area, but has no effect on the rise-decay symmetry nor on the peak-trough symmetry.

References

Tadel F, Baillet S, Mosher JC, Pantazis D, Leahy RM. Brainstorm: A User-Friendly Application for MEG/EEG Analysis. Computational Intelligence and Neuroscience, vol. 2011, Article ID 879716, 13 pages, 2011. doi:10.1155/2011/879716

Gramfort, M. Luessi, E. Larson, D. Engemann, D. Strohmeier, C. Brodbeck, R. Goj, M. Jas, T. Brooks, L. Parkkonen, M. Hämäläinen, MEG and EEG data analysis with MNE-Python, Frontiers in Neuroscience, Volume 7, 2013, ISSN 1662-453X, [DOI]

Kamarajan, C., Porjesz, B., Jones, K. A., Choi, K., Chorlian, D. B., Padmanabhapillai, A., ... & Begleiter, H. (2004). The role of brain oscillations as functional correlates of cognitive systems: a study of frontal inhibitory control in alcoholism. International Journal of Psychophysiology, 51(2), 155-180.

Leventhal, D. K., Gage, G. J., Schmidt, R., Pettibone, J. R., Case, A. C., & Berke, J. D. (2012). Basal ganglia beta oscillations accompany cue utilization. Neuron, 73(3), 523-536.

Engel, A. K., & Fries, P. (2010). Beta-band oscillations—signalling the status quo?. Current opinion in neurobiology, 20(2), 156-165.

Holt, A. B., Kormann, E., Gulberti, A., Pötter-Nerger, M., McNamara, C. G., Cagnan, H., ... & Westphal, M. (2019). Phase-dependent suppression of beta oscillations in Parkinson's disease patients. *Journal of Neuroscience*, *39*(6), 1119-1134.

Lundqvist, M., Herman, P., Warden, M. R., Brincat, S. L., & Miller, E. K. (2018). Gamma and beta bursts during working memory readout suggest roles in its volitional control. *Nature communications*, *9*(1), 394.

Schmidt, R., Ruiz, M. H., Kilavik, B. E., Lundqvist, M., Starr, P. A., & Aron, A. R. (2019). Beta Oscillations in Working Memory, Executive Control of Movement and Thought, and Sensorimotor Function. *Journal of Neuroscience*, *39*(42), 8231-8238.

Wagner, J., Wessel, J. R., Ghahremani, A., & Aron, A. R. (2018). Establishing a right frontal beta signature for stopping action in scalp EEG: implications for testing inhibitory control in other task contexts. *Journal of cognitive neuroscience*, *30*(1), 107-118.

Gerber, E. M., Sadeh, B., Ward, A., Knight, R. T., & Deouell, L. Y. (2016). Non-sinusoidal activity can produce cross-frequency coupling in cortical signals in the absence of functional interaction between neural sources. *PloS one*, *11*(12), e0167351.

Lozano-Soldevilla, D., ter Huurne, N., & Oostenveld, R. (2016). Neuronal oscillations with non-sinusoidal morphology produce spurious phase-to-amplitude coupling and directionality. *Frontiers in computational neuroscience*, *10*, 87.

Lundqvist, M., Rose, J., Herman, P., Brincat, S. L., Buschman, T. J., & Miller, E. K. (2016). Gamma and beta bursts underlie working memory. *Neuron*, *90*(1), 152-164.

Aron, A. R., Robbins, T. W., & Poldrack, R. A. (2014). Inhibition and the right inferior frontal cortex: one decade on. *Trends in cognitive sciences*, *18*(4), 177-185.

Figures

Figure 1

Peaks, troughs and midpoints

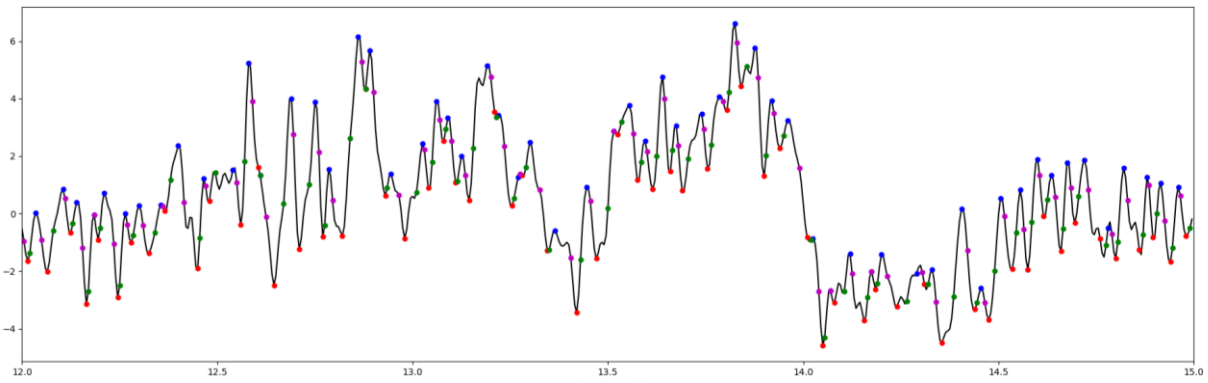

Note: Example of the identification of the peaks, troughs, and midpoints of the rise and decay flanks of the epoched signal of the prefrontal central sensor when a deviant tone was presented.

Figure 2

Burst detection and applied thresholds

A

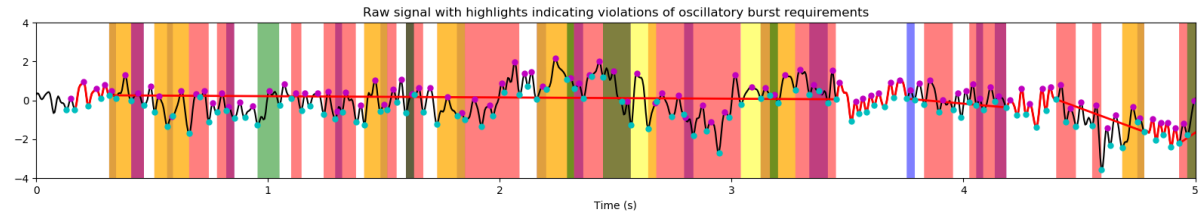

B

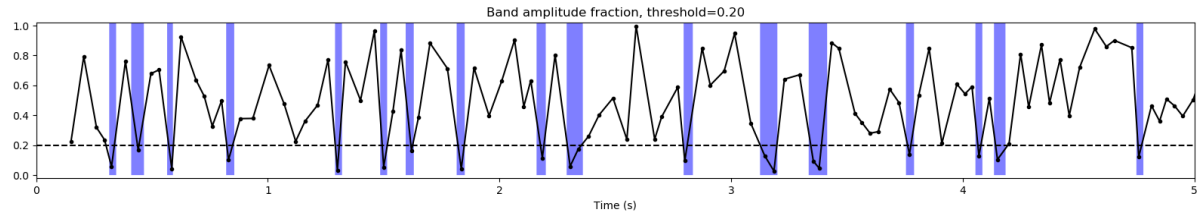

C

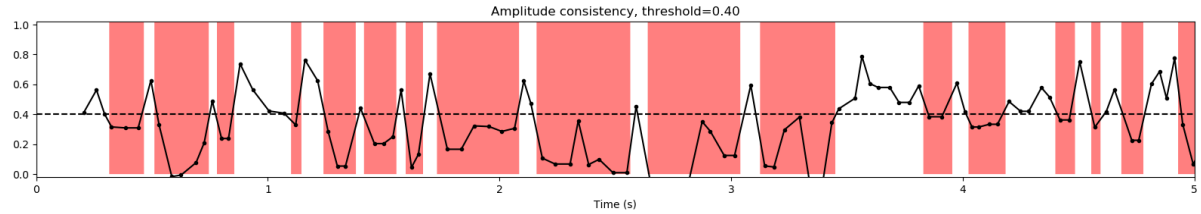

D

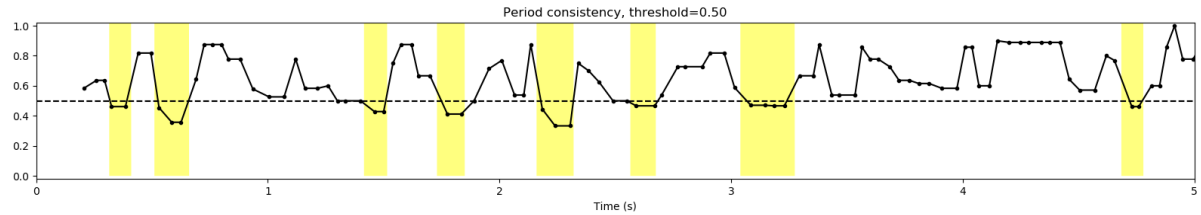

E

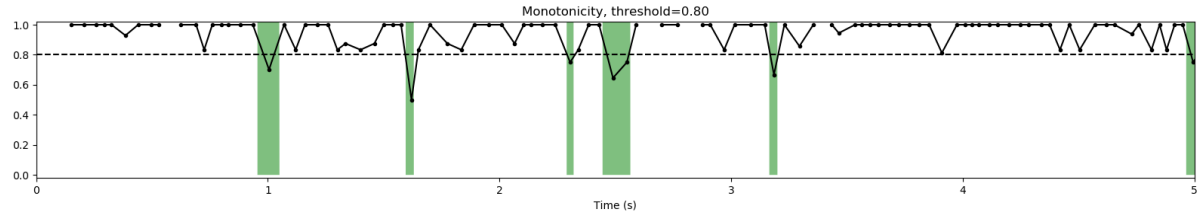

Note: Example of burst detection in prefrontal central sensor. A, Shows the cycle which exceed the set thresholds and are defined as a oscillatory burst. B, shows the cycles (blue) which do not exceed the amplitude fraction threshold (0.2). C, show the cycles (red) which do not exceed the amplitude consistency threshold (0.4). D, shows the cycles (yellow) which do not exceed the period consistency threshold (0.5). E, shows the cycles (green) which do not exceed the monotonicity threshold (0.8).

Figure 3

Comparison pre- and post-cue

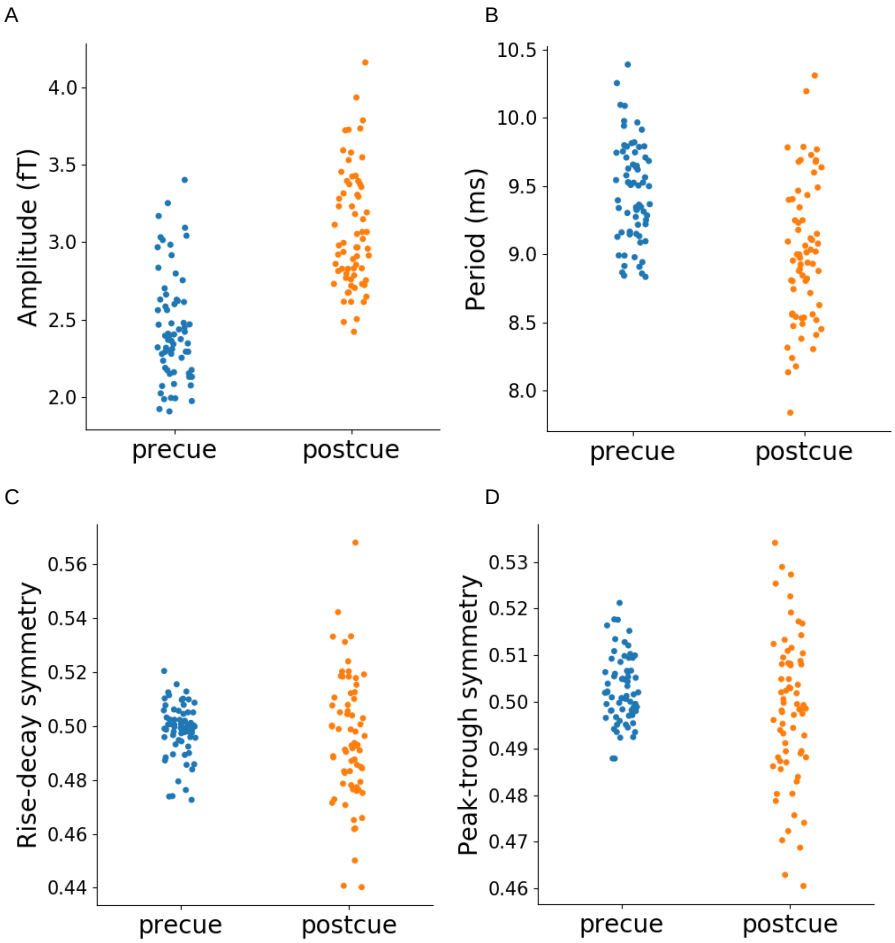

Note: visualization of the differences in oscillation features. A, Differences in amplitude (fT) of beta oscillation before (blue) and after (orange) the presentation of the deviant tone. B, Differences in periods (ms) of beta oscillation before (blue) and after (orange) the presentation of the deviant tone. C, Differences in rise-decay symmetry of beta oscillation before (blue) and after (orange) the presentation of the deviant tone. D, Differences in peak-trough symmetry of beta oscillation before (blue) and after (orange) the presentation of the deviant tone.

Figure 4

Comparison frontal and occipital sensors

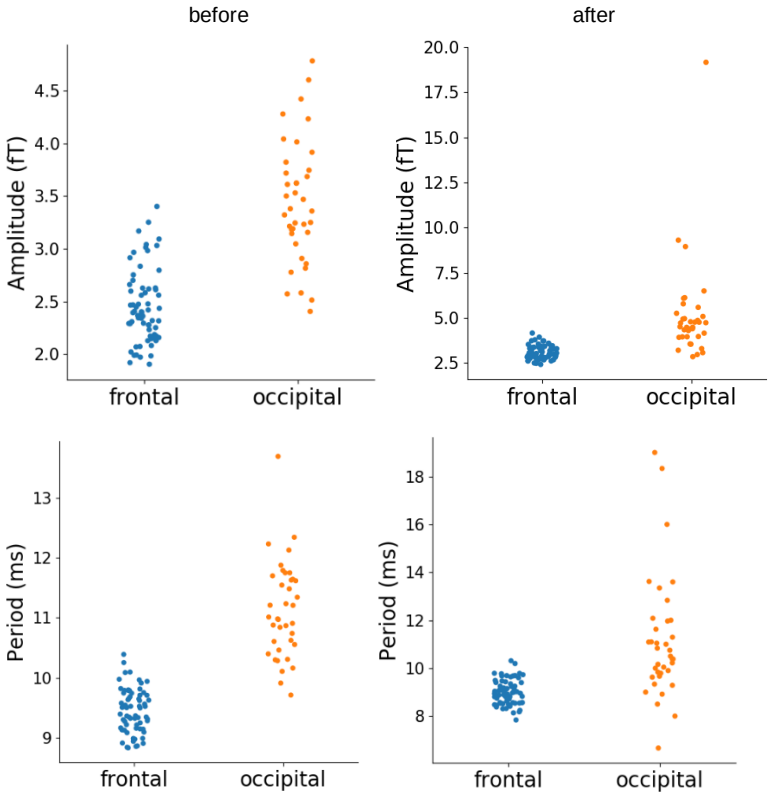

Note: visualization of differences in amplitude (A) and period (B) in frontal (blue) and occipital (orange) before and after the presentation of the deviant tone.

Figure 5

Visual comparison of cycle-by-cycle and dual amplitude

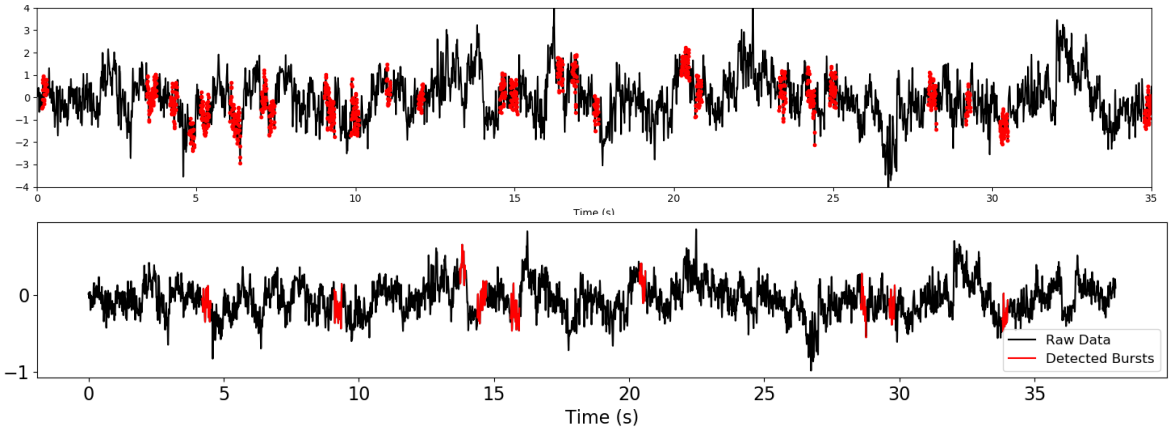

Note: Example of burst detection by the cycle-by-cycle algorithm (above) and dual-amplitude threshold (below) of the central prefrontal sensor.